Submitted to the Annals of Applied Statistics

BAYESIAN NONPARAMETRIC MULTIVARIATE SPATIAL MIXTURE MIXED EFFECTS MODELS WITH APPLICATION TO AMERICAN COMMUNITY SURVEY SPECIAL TABULATIONS

BY RYAN JANICKI[1], ANDREW M. RAIM[1,*] SCOTT H. HOLAN[2,3,‡] AND JERRY MAPLES[1,†]

[1]*Center for Statistical Research and Methodology, U. S. Census Bureau, ryan.janicki@census.gov,* [*]*andrew.raim@census.gov,* [†]*jerry.j.maples@census.gov*

[2]*Office of the Associate Director for Research and Methodology, U. S. Census Bureau*

[3]*Department of Statistics, University of Missouri,* [‡]*holans@missouri.edu*

Leveraging multivariate spatial dependence to improve the precision of estimates using American Community Survey data and other sample survey data has been a topic of recent interest among data-users and federal statistical agencies. One strategy is to use a multivariate spatial mixed effects model with a Gaussian observation model and latent Gaussian process model. In practice, this works well for a wide range of tabulations. Nevertheless, in situations in which the data exhibit heterogeneity within or across geographies, and/or there is sparsity in the data, the Gaussian assumptions may be problematic and lead to underperformance. To remedy these situations, we propose a multivariate hierarchical Bayesian nonparametric mixed effects spatial mixture model to increase model flexibility. The number of clusters is chosen automatically in a data-driven manner. The effectiveness of our approach is demonstrated through a simulation study and motivating application of special tabulations for American Community Survey data.

1. Introduction. The American Community Survey (ACS) is the largest household survey run by the U.S. Census Bureau. The ACS is an ongoing survey which samples approximately 3.5 million households annually spread-out through the year and collects data on a broad range of social, demographic, economic, and housing characteristics.[1] The ACS annually produces a large number of tables at various levels of aggregation. Specifically, the ACS produces both 1-year and 5-year period estimates depending on the population for different geographies. The one-year period estimate is derived over a single calendar year for geographical areas with a population of at least 65,000. In contrast, for all geographical areas down to the tract level, table estimates are also produced aggregating 5 years of survey data (also known as 5-year period estimates); e.g., the 2018 5-year ACS estimates will be tabulated using respondents from January 2014 to December 2018. The Census Bureau also produced 3-year period estimates for geographies with populations between 20,000 and 65,000, though these estimates were discontinued in 2013 (https://www.census.gov/programs-surveys/acs/guidance/estimates.html).

The U.S. Census Bureau publishes tables using 5-year ACS estimates for many social, demographic, and economic cross-classifications, when the sample sizes are sufficiently large for the published estimates to be considered reliable, and to not pose a risk of disclosure of a respondent's personal identifying information. In addition to the standard tables released by the U.S. Census Bureau, stakeholders have requested custom statistical data products known as *special tabulations*, which are more detailed than publicly available tables. For example,

Keywords and phrases: American Community Survey, Dirichlet process, Mixture models, Nonparametric Bayes, Small area estimation.

[1]For more details see http://www.census.gov/acs.

the Minnesota Department of Education requested a tabulation to help administer programs for early childhood development. This tabulation is associated with a finer breakdown of children's ages into age groups (0–1, 2–3, 4–5) crossed by race, income level, Hispanic origin, or relationship to householder (individually, not jointly) for every county in Minnesota. Many of these tables have cells with very few or no survey cases, resulting in issues of data quality and/or disclosure limitations. From a data quality perspective[2], estimates which only use the direct survey data based on a small sample size may lack precision or may not be possible at all (Rao and Molina, 2015). Releasing estimates based on small sample sizes also increases the risk of unintended disclosures for responding individuals.

The mission of the Census Bureau is to provide accurate official statistics using data collected by its programs, but also to ensure that privacy and confidentiality of respondents is protected. For this reason, the release of special tabulations products was significantly curtailed, and the agency is considering alternatives to releasing the direct survey estimates. The Census Bureau is beginning to incorporate techniques from the differential privacy literature which offer mathematical guarantees on privacy (Abowd, 2018). There has been a large-scale and ongoing effort to develop innovative methods to protect releases of major Census Bureau data products. This work considers a more immediate solution, which is to produce model-based predictions, based on the direct estimates, for release by the agency. Because model-based predictions are indirect estimates which utilize the entire dataset, the individual disclosure risk is greatly reduced, albeit without the mathematical guarantees of differential privacy.

Latent Gaussian process (LGP) models have become a standard tool for modeling dependencies in count-valued and other non-Gaussian datasets, see Diggle, Tawn and Moyeed (1998). A natural approach to implementing LGP models is through hierarchical statistical modeling and, in particular, using a Bayesian formulation. In this context, the joint distribution of the data, latent processes, and unknown parameters are written as the product of a data model, a Gaussian process model, and a parameter model (e.g., see Cressie and Wikle (2011); Banerjee, Carlin and Gelfand (2014), among others). Within this model framework, complex dependencies based on the multivariate structure of the outcome, spatial and temporal relationships, and their interactions, can be incorporated. Efficient estimation of the joint posterior distribution of the process and parameters given the data then proceeds through an application of Bayes theorem.

Many models used in small area estimation (SAE) exist within this class of LGP models, e.g. the Fay-Herriot model (Fay and Herriot, 1979) and its extensions; see Bradley, Holan and Wikle (2015) for additional discussion. The LGP class of models is highly flexible. They can include many types of relationships in the data and provide a useful tool for 'borrowing strength,' using multivariate, spatial and/or temporal dependencies, to improve estimates that lack sufficient survey data.

Another complexity of the data is that some tabulations may not result from a singular spatial pattern, but instead may result from the aggregate of several. In other words, modeling the distribution of tabulated values may not conform to an underlying known parametric distribution. For example, preliminary analysis of the age by race table suggested that there were different spatial patterns for different racial groups across the counties. To address this data complexity, we propose a Bayesian nonparametric mixture of LGP models. Sections 4 and 6 will explore this further. Importantly, one of the primary motivations of our approach is to produce a flexible model that could be readily utilized in a production environment without having to determine a rich set of covariates for different tabulations.

[2]The Census Bureau's statistical quality standards for published survey estimates (Section F1-6) can be viewed at https://www.census.gov/about/policies/quality/standards.html.

Related work is that of Gelfand, Kottas and MacEachern (2005), who introduced Dirichlet process mixing for spatial point process models. Gelfand, Kottas and MacEachern (2005) used the Dirichlet process prior for the purpose of developing a framework for the analysis of non-Gaussian, nonstationary, point-referenced spatial data. In contrast, the current work is concerned with analysis of multivariate spatial areal data collected from a sample survey. We combine elements of small area estimation theory (Rao and Molina, 2015), multivariate spatial distribution theory (Bradley, Holan and Wikle, 2015), and Bayesian nonparametrics (Hjort et al., 2010) for the purpose of producing flexible model-based predictions of area-level means with greater precision than those of the direct, survey-based estimates. There are several other contributions to the literature for Bayesian nonparametric data for spatial data. For example, see Fernández and Green (2002), Duan, Guindani and Gelfand (2007), Hossain et al. (2013), Neelon, Gelfand and Miranda (2014), Reich and Fuentes (2015), Kottas (2016), Hosseinpouri and Khaledi (2019), among others, though these primarily focus either on univariate models and/or point-level data. Consequently, we introduce a Dirichlet process prior on the latent Gaussian process, primarily for the purpose of clustering the observed data on multivariate characteristics and on similar spatial patterns.

The remainder of this paper is organized as follows. In Section 2, we describe multivariate spatial mixed effects models (MSM) and their application to the ACS. In Section 3, we present results of fitting the MSM to two different 5-year ACS special tabulations. In Section 3.1 we fit the MSM to ACS 5-year estimates of the number of children by age in counties in Minnesota, and show good performance of model-based estimates, compared to the corresponding direct, survey-based estimates. In Section 3.2, we show that for certain special tabulations, the MSM can produce predictions of obvious poor quality when the data exhibit heterogeneous spatial and multivariate patterns. As an example, the MSM is fit to ACS 5-year estimates of the number of children in counties by age and race in counties in Minnesota. To remedy such problems, an extension to the MSM is proposed in Section 4, which introduces the multivariate spatial mixed effects model with Dirichlet process mixing (MSMM). An empirical simulation study is provided in Section 5 and illustrates the effectiveness of our proposed modeling approach. In Section 6, we fit the MSMM to the age by race dataset, and show good performance of the predictions, compared to the predictions from the MSM or the direct estimates. Concluding remarks are given in Section 7.

2. Multivariate Spatial Mixed Effects Model. Conceptually, special tabulations and other ACS data are a collection of multi-way contingency tables for a set of areas in a given geographical domain. For example, one particular tabulation concerns the counts of children in three groups: 0–1, 2–3, and 4–5 years of age. A one-way table with counts of the three age groups is constructed for each county in the United States. A second tabulation provides counts of children in the same three age groups, but also cross-classified by a race factor with seven categories: White alone, Black alone, Asian alone, American Indian or Alaska Native alone, Native Hawaiian or Pacific Islander alone, Other alone, or two or more races. Here, a two-way table is constructed for each county. These are just two examples of many special tabulations of ACS data that the U.S. Census Bureau is tasked with producing; others include cross-classifications of demographic characteristics (e.g. age, race, gender, income), different housing characteristics (e.g. owner vs. renter) and geographic regions (e.g. states, counties, and tracts).

In general, suppose there are k factors in a particular table under consideration, where the levels of the jth factor are indexed by $i_j = 1, \ldots, I_j$. Excluding marginal counts, which are typically provided with the data, let L denote the number of interior table cells. In this work, factors are crossed so that $L = I_1 \times \cdots \times I_k$; however, in principle, factors may also be nested so that certain levels of one factor are defined only for some levels of other factors.

Let $\mathcal{D}$ denote the collection of geographies currently under consideration, writing $A \in \mathcal{D}$ to represent a particular areal unit within the domain. Each table consists of direct estimates based on the Horvitz-Thompson estimator

$$Z^{*(l)}(A) = \sum_{j \in \mathcal{S}^{(l)}(A)} w_j, \tag{1}$$

where $j \in \mathcal{S}^{(l)}(A)$ are the sampled units belonging to interior table cells $l = 1, \ldots, L$ and areas $A \in \mathcal{D}$, and w_j is the associated survey weight. Let $D^{*(l)}(A)$ be an estimate of the design-based variance of $Z^{*(l)}$; the U.S. Census Bureau uses the successive differences replication method (Judkins, 1990; Fay and Train, 1995; Torrieri, 2014). Therefore, the multivariate observation $\{\left(Z^{*(l)}(A), D^{*(l)}(A)\right) : l = 1, \ldots, L\}$ represents a table of direct estimates for area A. Let $m = |\mathcal{D}|$ denote the number of areal units so that $n = mL$ is the total number of observations in the tabulation. To facilitate modeling estimates of counts, which are likely to be right-skewed, we transform the direct estimates (1) using

$$Z^{(l)}(A) = \log\left(Z^{*(l)}(A) + 1\right), \tag{2}$$

adding one due to the presence of direct estimates with a value of zero. Let $D^{(l)}(A)$ be the variance estimate of the log-transformed direct estimate, $Z^{(l)}(A)$.

To produce model-based estimates of the direct ACS estimates, we must formulate an appropriate model. Because the data represent entries of spatially-dependent contingency tables, we consider a multivariate spatial mixed effects model (MSM) which takes these dependencies into account. The model will now be formulated via the standard data, process, parameter model formulation popularized in the spatial statistics literature (Cressie and Wikle, 2011). The data model is defined as

$$Z^{(l)}(A) = Y^{(l)}(A) + \varepsilon^{(l)}(A), \tag{3}$$

for $A \in \mathcal{D}$ and $l = 1, \ldots, L$. Survey estimates $Z^{(l)}(A)$ are assumed to be design unbiased estimates of the underlying population quantities $Y^{(l)}(A)$. The survey design is incorporated via sampling error terms, $\varepsilon^{(l)}(A)$, which are assumed to be independent, normally distributed, mean-zero random variables, with known sampling variances $D^{(l)}(A)$. The process model is given by

$$Y^{(l)}(A) = \mu^{(l)}(A) + \nu^{(l)}(A), \tag{4}$$

where $\mu^{(l)}(A)$ is an unknown fixed effect representing the large-scale multivariate spatial trend. The term $\nu^{(l)}(A)$ is a random effect used to incorporate multivariate spatial dependencies in the process model and accounts for any large-scale residual spatial dependence. The fixed effects, $\mu^{(l)}(A)$, are modeled using a linear regression, $\mu^{(l)}(A) = \boldsymbol{x}^{(l)}(A)^\top \boldsymbol{\beta}$, where $\boldsymbol{x}^{(l)}(A)$ is a p-dimensional vector of known covariates, and $\boldsymbol{\beta}$ is a p-dimensional vector of unknown regression coefficients. Denote $\boldsymbol{X}$ as an $n \times p$ design matrix whose rows consist of the $\boldsymbol{x}^{(l)}(A)$. Prediction of the latent process, $Y^{(l)}(A)$, from the observed data, $Z^{(l)}(A)$, is the primary interest in fitting the model. After model fitting, the inverse transformation

$$Y^{*(l)}(A) = e^{Y^{(l)}(A)} - 1 \tag{5}$$

can be applied to obtain predictions and measures of uncertainty on the original scale.

REMARK 2.1. In the spatial literature, but not necessarily in the small area estimation literature, it is common to model the random process, $Y^{(l)}(A)$, using an additional fine-scale variability term, $\xi^{(l)}(A)$, so that the process model becomes

$$Y^{(l)}(A) = \mu^{(l)}(A) + \nu^{(l)}(A) + \xi^{(l)}(A),$$

where, in many cases, $\xi^{(l)}(A) \overset{\text{i.i.d.}}{\sim} \mathrm{N}(0, \sigma^2_\xi)$. The term $\xi^{(l)}(A)$ is used to describe the local behavior of the process $Y^{(l)}(A)$. In the work presented here, fitting a spatial model that includes the fine-scale variability terms for the ACS data resulted in overfitting, so that predictions and uncertainty estimates were largely the same as the survey-based estimates. It is possible that the sampling variances in the data model largely account for any residual fine-scale variability, so that inclusion of the additional terms, $\xi^{(l)}(A)$, result in a weakly identifiable model. In addition, at the level of geographies often considered, when constructing tabulations for public dissemination (county-level), the spatial variation is generally smooth and can be accounted for through the other terms in the model. When using the process model in (4), we found no issues with overfitting. ■

The random effects, $\nu^{(l)}(A)$, are modeled using a basis expansion,

$$\nu^{(l)}(A) = \boldsymbol{\psi}^{(l)}(A)^\top \boldsymbol{\eta},$$

where the $\boldsymbol{\psi}^{(l)}(A)$ are r-dimensional multivariate spatial basis functions and the distribution of the random coefficient $\boldsymbol{\eta}$ is specified to capture spatial dependencies in the data. Taking $r \ll n$ has the effect of inducing sparsity and reducing the rank of the model, which leads to a more parsimonious model, drastically reducing the computational burden of fitting the model, particularly when fitting to very large datasets (Hughes and Haran, 2013). Also, when $r \ll n$, multiple observations will share common elements of the random coefficient vector $\boldsymbol{\eta}$ in this model specification, inducing multivariate dependence.

The vectors $\boldsymbol{\psi}^{(l)}(A)$ can be any set of multivariate spatial basis functions (see Bradley, Wikle and Holan, 2017). However, following Hughes and Haran (2013) and Bradley, Holan and Wikle (2015), we use the Moran's I basis functions, which are chosen to avoid confounding between the fixed effects and the random effects. Let $\boldsymbol{A}$ be an $n \times n$ multivariate adjacency matrix corresponding to areal units $A \in \mathcal{D}$; specifically, $\boldsymbol{A} = \boldsymbol{W} \otimes \mathbf{1}_L \mathbf{1}_L^\top$ where $\otimes$ represents the Kronecker product, $\mathbf{1}_L$ is an $L \times 1$ matrix of ones, and $\boldsymbol{W} = (w_{ii'})$ is a standard adjacency matrix defined by

$$w_{ii'} = \begin{cases} 0 & \text{if } i = i', \\ 1 & \text{if } i \neq i' \text{ and areas } i \text{ and } i' \text{ are adjacent}, \\ 0 & \text{otherwise}, \end{cases}$$

for $i, i' \in \{1, \ldots, m\}$. The Moran's I (MI) operator (Moran, 1950) is given by

$$G(\boldsymbol{X}, \boldsymbol{A}) \equiv (\boldsymbol{I}_n - \boldsymbol{X}(\boldsymbol{X}^\top \boldsymbol{X})^{-1} \boldsymbol{X}^\top) \boldsymbol{A} (\boldsymbol{I}_n - \boldsymbol{X}(\boldsymbol{X}^\top \boldsymbol{X})^{-1} \boldsymbol{X}^\top). \tag{6}$$

The multivariate spatial basis functions $\boldsymbol{\psi}^{(l)}(A)$ are defined to be the r eigenvectors corresponding to the r largest positive eigenvalues of the $n \times n$ matrix $G(\boldsymbol{X}, \boldsymbol{A})$ (Hughes and Haran, 2013). We then define $\boldsymbol{\Psi}$ to be the $n \times r$ matrix with rows $\boldsymbol{\psi}^{(l)}(A)$. Although $\boldsymbol{\Psi}$ only needs to be computed once for a given $\boldsymbol{X}$ and $\boldsymbol{A}$, time and memory requirements to naïvely compute the spectral decomposition can become impractical for large n encountered in modeling special tabulations. Specialized software libraries are available to compute only the requested eigenvectors (e.g. Qiu and Mei, 2019). This work uses a form of $\boldsymbol{X}$ which admits a lower dimensional computation; see Section 3 and the Supplementary Materials for details.

We assume $\boldsymbol{\eta} \sim \mathrm{N}_r(\mathbf{0}, \sigma^2_{\boldsymbol{\eta}} \boldsymbol{K})$, where $\boldsymbol{K}$ is a positive definite matrix chosen to induce a conditional autoregressive structure on the random effects, $\nu^{(l)}(A)$. The variance component, $\sigma^2_{\boldsymbol{\eta}}$, is an unknown parameter to be estimated. Let $\boldsymbol{Q}$ be the singular, positive semi-definite precision matrix for an intrinsic conditional autoregressive (ICAR) process. That is,

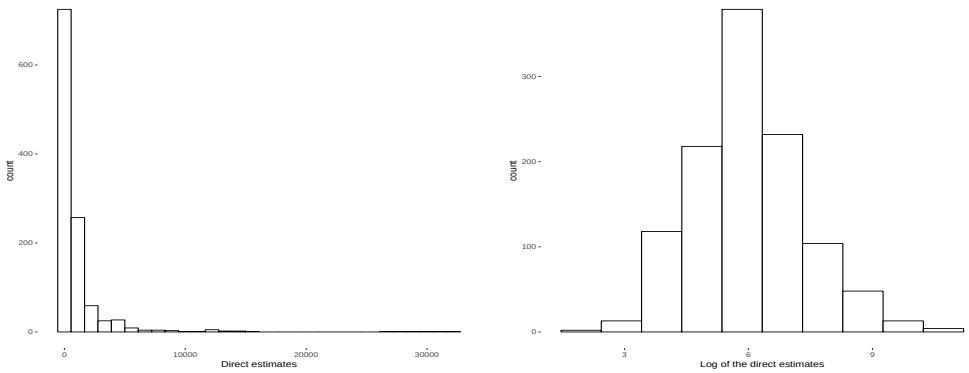

(a) Histogram of the ACS 5 year estimates of total children, ages 0–1, 2–3, and 4–5, in counties in Midwestern states

(b) Histogram of the log of the ACS 5 year estimates of total children, ages 0–1, 2–3, and 4–5, in counties in Midwestern states

Fig 1: Comparison of the distribution of estimates of counts with the distribution of the estimates of the log of counts.

$\boldsymbol{Q} = \boldsymbol{D} - \boldsymbol{A}$, where $\boldsymbol{D}$ is a diagonal matrix, with diagonal entries equal to the row sums of $\boldsymbol{A}$. Following Hughes and Haran (2013), let $\boldsymbol{K}^{-1} = \boldsymbol{\Psi}^\top \boldsymbol{Q} \boldsymbol{\Psi}$. It can be shown that $\boldsymbol{K}^{-1}$ is positive definite, so long as $\boldsymbol{X}$ includes an intercept (Porter, Holan and Wikle, 2015). Bradley, Holan and Wikle (2015) shows that this specification of the precision matrix $\boldsymbol{K}^{-1}$ minimizes the Frobenious norm $\|\boldsymbol{Q} - \boldsymbol{\Psi} \boldsymbol{C}^{-1} \boldsymbol{\Psi}^\top\|_{\mathrm{F}}$ over $\boldsymbol{C}$ in the space of positive definite $r \times r$ matrices. In this sense, $\boldsymbol{K}^{-1}$ is the best positive approximant to the ICAR precision matrix $\boldsymbol{Q}$ (Higham, 1988).

The model specification is completed by choosing parameter models for the unknown parameters, $\boldsymbol{\beta}$ and $\sigma^2_{\boldsymbol{\eta}}$. Using independent priors, $\boldsymbol{\beta} \sim \mathrm{N}_p(\boldsymbol{0}, \sigma^2_{\boldsymbol{\beta}} \boldsymbol{I}_{p \times p})$, and $\sigma^2_{\boldsymbol{\eta}} \sim \mathrm{IG}(a, b)$, leads to full conditional distributions from known parametric families, allowing for easy sampling from the posterior distribution. See the Supplementary Materials for derivation of the full conditional distributions.

3. Application of MSM to ACS Special Tabulations. The MSM model from Section 2 can be a useful tool for producing model-based special tabulations of ACS data. Model-based predictions may be significantly more accurate than associated ACS direct estimates for certain demographic and geographic cross-classifications of ACS data. However, MSM predictions for some tabulations can be of extremely poor quality. In this section, we consider MSM for two particular tabulations. Section 3.1 models total number of children by age group. Section 3.2 models total number of children by the cross-classification of both age group and race. Both tabulations are for counties in Minnesota, and are based on 2015 ACS 5-year data. The 2015 5-year ACS data consists of pooled ACS data over the period 2011–2015, with survey weight adjustments made to reflect the different time periods in which data were collected. The advantage of using 5-year data over 1-year ACS data is the larger sample sizes available, and that 5-year data is publicly available for a wider range of geographies and economic and demographic variables than 1-year data.

We find that MSM can produce high quality predictions in the situation of Section 3.1, with model-based predictions having greatly reduced standard errors, relative to the direct estimates. We have also found (but not included in the paper) that MSM can produce high quality predictions when applied to certain cross-classifications such as age by poverty status,

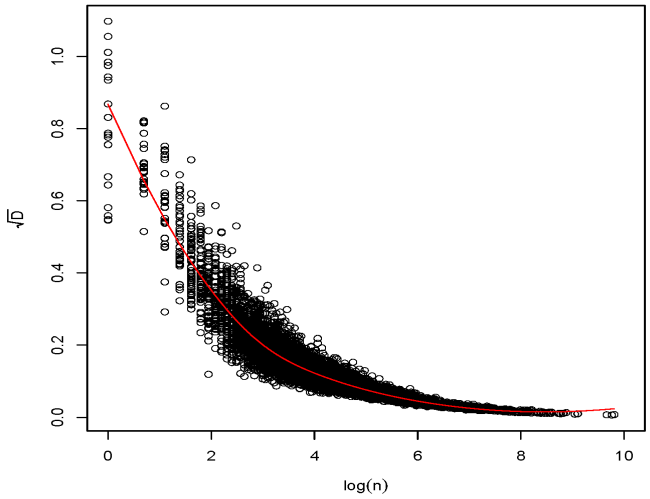

Fig 2: Scatter plot of the estimated standard errors of the direct estimates of the log counts of children, ages 0–1, 2–3, or 4–5, in counties in Minnesota and surrounding states, vs. the log of the sample sizes. The red line shows the fit of a LOESS regression of the direct estimates of the log counts on the log of the county sample sizes.

age by gender, and age by housing composition using similar datasets. However, poor predictions from the fitted MSM model could occur when the dimension of the special tabulations increased, when the number of cross-classifications of interest increased, or when—even with relatively simple multivariate tabulations—the underlying spatial field assumed by the model was inappropriate. This situation is illustrated in Section 3.2.

3.1. *Estimation of the number of children in counties in Minnesota.* We first consider fitting a special tabulation of one-way contingency tables containing counts of children in categories 0–1, 2–3, and 4–5 years of age for counties in Minnesota. Within counties, there is strong positive correlation of direct estimates of total children in the three age categories. Exploratory analysis using Moran's I statistic (Moran, 1950) on each marginal dataset also indicated strong spatial correlation in the data.

Figure 1a shows a histogram of the direct estimates of total children in counties in the 0–1, 2–3, and 4–5 age groups. Before applying transformation (2) the distribution of the direct estimates is heavily right skewed due to the presence of counties with large cities. Figure 1b shows the histogram of the transformed direct estimates; this suggests modeling the direct estimates on the log scale using the multivariate spatial model.

The sampling variances of the direct estimates are also needed as model inputs. For the nonzero direct estimates, the method of replicate weights can be used to estimate the sampling variances (Judkins, 1990). However, the presence of direct estimates of zero introduces an additional challenge, due to the fact that there is no way to directly estimate their sampling variances. To overcome this difficulty, a generalized variance function is used. Figure 2 shows a scatter plot of the estimated sampling variances versus the log of the sample sizes for the nonzero direct estimates. For the areas where the estimated sampling variances are not defined, a plug-in estimate from the displayed LOESS smoothing curve is used in the model.

While the goal is estimation of counts in counties in Minnesota, we fit the model to data from counties in Minnesota, as well as counties in the surrounding states of Wisconsin, Iowa,

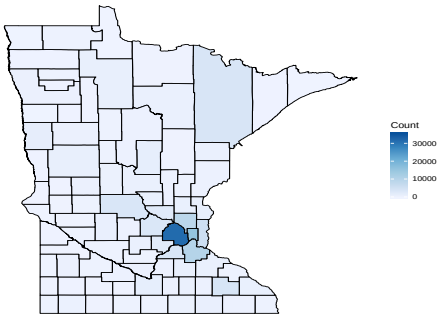

(a) Direct estimates of the number of children, ages 0–1.

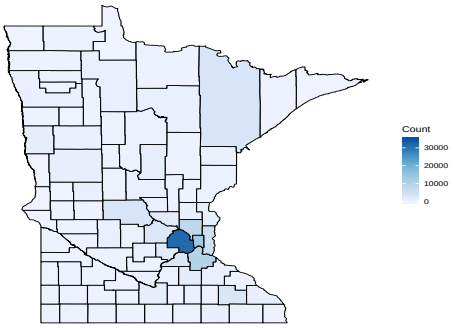

(b) Model-based predictions of the number of children, ages 0–1.

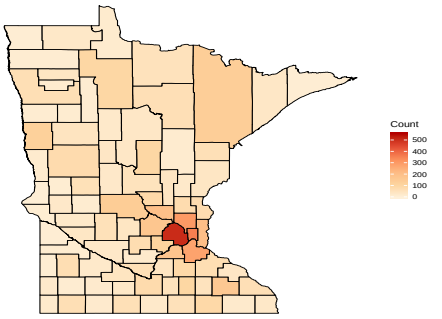

(c) Standard errors of direct estimates of the number of children, ages 0–1.

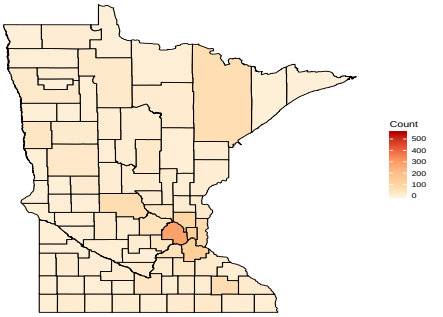

(d) Posterior standard error of model-based predictions of the number of children, ages 0–1.

Fig 3: Comparison of the spatial patterns of the direct estimates and the predicted values, in blue, and a comparison of the spatial patterns of the standard errors of the direct estimates and predicted values, in red.

North Dakota, and South Dakota. Expanding the set of areal units to the counties in surrounding states resulted in greater precision of predicted values, as the spatial field seemed to be more easily identified with an expanded number of spatial regions. We also investigated expanding the number of included areal units to all counties in the continental United States. However, this drastically increased the computational time needed to fit the model, without noticeably changing the predictions. We found expanding the set of areal units to include only counties in adjacent states to be a good tradeoff, in terms of reducing computational burden while maintaining stability of predictions.

The covariate, $\boldsymbol{x}^{(l)}(A)$, used in the model includes an intercept, the log of the county total population for area A, which is assumed known from Census population estimates, and indicator variables encoding the combination of factors for entry l of the original contingency table. In this case, $l = 1, 2, 3$ corresponds to age groups 0–1, 2–3, and 4–5.

The choice of the number of basis functions to use in the model specification remains an open question. Using too few basis functions can result in the model oversmoothing the data, while increasing the number of basis functions can add additional variance and computational burden. However, a careful choice of a reduced rank set of basis functions can be

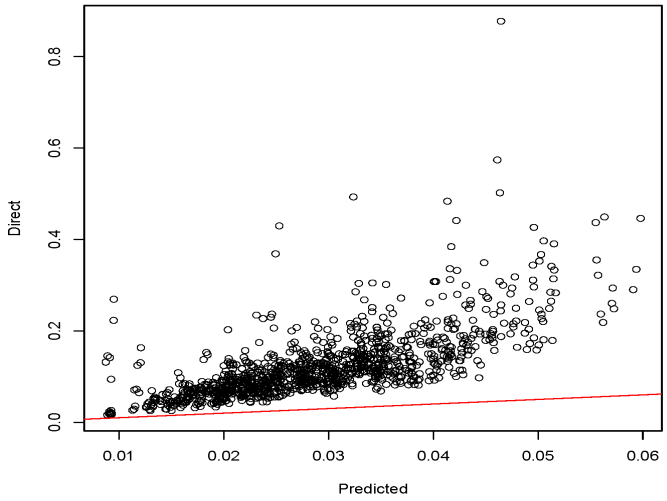

Fig 4: Comparison of the coefficients of variation of the predicted values vs. the coefficients of variation of the direct estimates, for all three margins: children ages 0–1, 2–3, and 4–5, for all counties in the Midwest. The diagonal line is shown in red.

shown to produce better predictions than those using a full set of basis functions (Bradley, Holan and Wikle, 2015). We present results from fitting the model using 36 basis functions, which is approximately 50% of the available MI basis functions. In a sensitivity study, we investigated the effects of varying the number of basis functions used. The predictions are relatively robust to changes in r, particularly when 50% or more of the available MI basis functions are used. When too few basis functions are included, the model can over smooth the data, and predictions for some of the small areas can have a higher bias. The tradeoff with using more basis functions is the increased computational burden of fitting the model. With the datasets analyzed in this project, a default of using 50% of the available MI basis functions seems to be a sensible choice.

We used the Stan modeling platform along with the RStan package (Stan Development Team, 2018) in R (R Core Team, 2019) to fit the multivariate spatial model to this ACS dataset. Stan worked very well in this example, as we were able to fit the model to this dataset using 2000 Hamiltonian Monte Carlo (HMC) iterations, using the first 1000 iterations as burn-in, in only a few minutes using a Windows laptop (Intel i7-6600U CPU @ 2.60GZ, 16GB of RAM). We used the package's built-in diagnostics to monitor convergence, with no issues detected. Draws of $Y^{*(l)}(A)$ are computed within a "generated quantities" block in Stan, yielding $Y_r^{*(l)}(A)$ for $r = 1, \ldots, R = 1000$ after HMC. Model-based predictions, variances, and standard errors are then taken to be

$$\hat{Y}^{*(l)}(A) = \frac{1}{R}\sum_{r=1}^{R} Y_r^{*(l)}(A), \quad \hat{D}^{(l)}(A) = \frac{1}{R-1}\sum_{r=1}^{R}\left[Y_r^{*(l)}(A) - \hat{Y}^{*(l)}(A)\right]^2, \tag{7}$$

and $[\hat{D}^{(l)}(A)]^{1/2}$, respectively.

Figure 3 compares the direct estimates with the model-based predictions of the number of children ages 0–1 in counties in Minnesota, and their associated standard errors. The direct estimates and model-based predictions are shown in blue in Figures 3a and 3b, respectively.

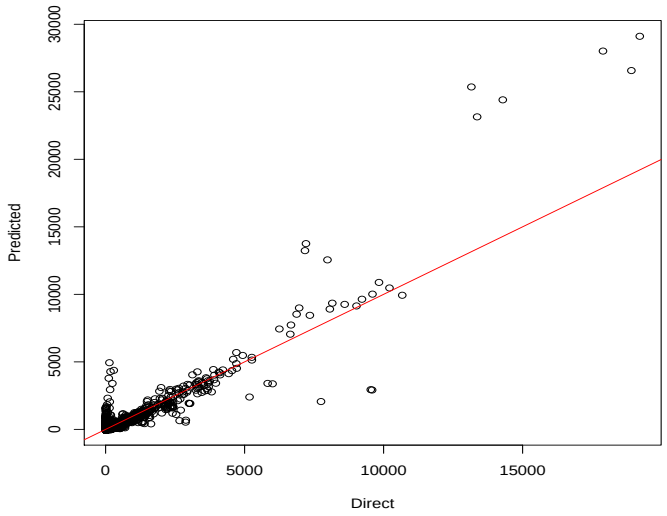

Fig 5: Comparison of the direct estimates and model-based estimates of the number of children in the 21 age by race groups in counties in Minnesota.

Here, it can be seen that the spatial patterns of the point estimates are very similar. Importantly, the model-based predictions are 'close' to the direct estimates in areas with large sample sizes, so that the model-based predictions preserve the direct estimates with low sampling variance. The predictions mainly differ from the direct estimates in areas with smaller sample size. In the areas with smaller sample size, the multivariate spatial model utilizes the spatial and multivariate correlation, to 'borrow information' across and within areas. A comparison of the standard errors of the direct estimates and model-based predictions is presented in Figures 3c and 3d. Here, as was seen with the point estimates, the spatial pattern of the standard errors is maintained. We also see significantly reduced standard errors in Figure 3d, compared to Figure 3c.

Figure 4 compares the coefficients of variation of the direct estimates with the coefficients of variation of the model-based predictions for all three margins: children ages 0–1, 2–3, and 4–5, for all counties in the Midwest. Here, we see a drastic increase in the precision of the model-based predictions over the corresponding direct estimates, with an overall average reduction in the coefficients of variation of approximately 73%. The improvement in precision, in this example, is uniform, with all counties seeing a reduction in the coefficient of variation of the model-based predictions. However, the most dramatic improvements in precision tend to be in the counties with smallest sample size. This is the 'borrowing of strength' phenomenon, which is often seen in small area estimation problems, where the effective sample size in small areas is increased by utilizing information from larger areas, thereby increasing precision of estimates. The preservation of spatial patterns of model-based predictions, along with an increase of precision of these point estimates has important policy consequences, as there is potential for more, and higher quality data releases, at possibly finer levels of geography than are currently available. Additional graphical comparisons of the direct estimates to model-based predictions using the multivariate spatial model can be found in the Supplementary Materials.

3.2. *Estimation of the number of children in counties in Minnesota by race.* We now fit the multivariate spatial model to direct estimates of the number of children, ages 0–1,

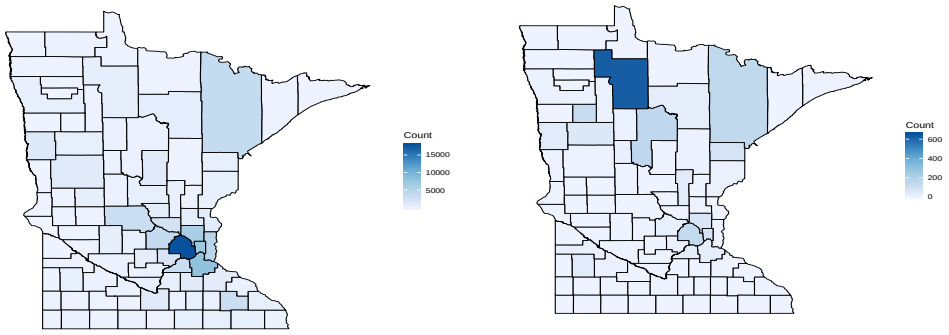

(a) Direct estimates of the number of White children, ages 2–3.

(b) Direct estimates of the number of American Indian or Alaska Native children, ages 2–3.

Fig 6: A comparison of the direct estimates of the number of White children, ages 2–3, with the direct estimates of the number of American Indian or Alaska Native children, ages 2–3, showing the varying spatial patterns on different margins within the multivariate data.

2–3, and 4–5 cross-classified by seven race categories, White Alone, Black Alone, Asian Alone, American Indian or Alaska Native Alone, Native Hawaiian or Pacific Islander alone, Other alone, or two or more races, in counties in Minnesota. The model specification and computational details, including covariates, priors, and MCMC methods, was the same as those used in the analysis in Section 3.1. Also, as in Section 3.1, we fit the model to direct estimates associated with counties in Minnesota, as well as surrounding Midwestern states.

Figure 5 shows a scatter plot of the predicted values in each of the 21 different age by race groups for each of the counties in Minnesota, against the corresponding direct estimates. While this type of plot is not a formal diagnostic for checking goodness of fit, it does give an indication of potential model failure. See also Molina, Nandram and Rao (2014), which includes many diagnostic scatter plots which are commonly used in small area estimation problems. Clearly the predicted values in Figure 5 are unacceptable, as some of the predicted values deviate from the direct estimates wildly. By construction, direct estimates are approximately design-unbiased. Hence, systematic patterns in the scatter plot away from the diagonal line give an indication of potential bias. At the upper right of Figure 5, we see predicted values of White children in some counties are nearly double the direct estimates. These direct estimates use the large sample sizes for counties containing large cities and are expected to be relatively precise, we would expect the associated predicted values to closely match the direct estimates. On the other end, in the lower left of Figure 5, we see direct estimates that are near zero, but with corresponding predicted values as much as 5,000, which in some cases is larger than the total number of people in that county. These observations taken together suggest large biases in the predicted values.

The reason for the large apparent biases in the predicted values can be inferred by looking at spatial plots of different margins of the tabulated ACS data. Figure 6 shows spatial plots of the age by race direct estimates for counties in Minnesota for two margins. Figure 6a shows the direct estimates of the number of White children, ages 2–3, and Figure 6b shows the direct estimates of the number of American Indian or Alaska Native children, ages 2–3. Clearly the spatial patterns in these two figures are quite different, with the largest number of White children estimated in to be in Hennepin County, which includes Minneapolis, while the greatest number of American Indian or Native American children are estimated to be in

the more rural, Beltrami County, in Northern Minnesota. In addition to the different spatial patterns, the scale of the margins of the data are very different, with the direct estimates of the number of White children ranging from 0–150,000, while the direct estimates of the number of American Indian or Alaska Native children range from 0–600, in this dataset.

The varying spatial patterns shown in Figure 6, and the resulting model assumption violation, help explain the poor performance of the predicted values from the fitted multivariate spatial model in this example. The predicted values aggressively smooth the direct estimates based on a common assumed spatial field. The shared spatial random effects for the different margins of the data result in large apparent biases, as the fitted model seems to try to compromise between the different spatial patterns, multivariate characteristics of the data, and the different scales of the direct estimates. Reexamination of Figure 5 does suggest a clustering effect, with predictions falling far from the diagonal, appearing to cluster in 3 or 4 groups.

Exploiting the spatial dependence, as well as the multivariate dependence, present in the data by incorporating a multivariate spatial process into the model is critical for producing predictions which have reduced standard errors from the corresponding direct estimates. In separate analyses (not shown) in which data models with independent error terms (Model (11) in Section 5) were fit to ACS direct estimates, we did not observe meaningful increases in precision. However, a poorly specified process model with a common assumed spatial field, as appears to be the case in this example, results in predictions with potentially serious biases for certain areas. One strategy might be to expand the number of basis functions to allow more flexibility in the model to accommodate the different aspects of the data. However, in this example, this approach was unsuccessful. A second strategy is to subset the data into more homogeneous groups, and to fit the multivariate spatial model to each subset. The problem here is that it is not always apparent how to subset the data, particularly as the dimension of the data and the number of cross-classifications present in the special tabulations increase. It is more desirable to have a data-driven method to cluster the data for these high dimensional problems. In the next section we extend the multivariate spatial model, by introducing a mixture component into the process model, to accommodate more complicated datasets with varying multivariate spatial characteristics.

4. Multivariate Spatial Mixed Effects Model with Dirichlet Process Mixing. For analysis of multivariate datasets with potentially varying spatial patterns, it is of interest to develop model-based methods which can cluster the observed data according to common multivariate characteristics and common spatial patterns, in addition to producing precise area-level predictions. Also, for the reasons previously discussed, we may not have strong prior information about the number of clusters. It is therefore desirable to allow for uncertainty in the number of clusters that are used. The Dirichlet process (Ferguson, 1973) naturally incorporates these two properties.

For more complicated datasets, we introduce the following extension of the multivariate mixed effect spatial model, which incorporates Dirichlet process mixing on the latent Gaussian process and regression coefficients. As before, the data model is given by

$$Z^{(l)}(A) = Y^{(l)}(A) + \varepsilon^{(l)}(A),$$

for $l = 1, \ldots, L$ and $A \in \mathcal{D}$. Writing $\boldsymbol{\theta}^{(l)}(A)^\top = \left(\boldsymbol{\beta}^{(l)}(A)^\top, \boldsymbol{\eta}^{(l)}(A)^\top\right)$, the process model is now

$$\begin{aligned} Y^{(l)}(A) &= \boldsymbol{x}^{(l)}(A)^\top \boldsymbol{\beta}^{(l)}(A) + \boldsymbol{\psi}^{(l)}(A)^\top \boldsymbol{\eta}^{(l)}(A) \\ \boldsymbol{\theta}^{(l)}(A) \mid G &\sim G \\ G \mid \alpha, G_0 &\sim \mathrm{DP}(\alpha G_0), \end{aligned} \tag{8}$$

where DP(αG_0) represents a Dirichlet process (DP) prior, parameterized by the concentration parameter α and the base measure G_0. The DP prior is used as the clustering mechanism in the process model. Here, a cluster is characterized by observations $Y^{(l)}(A)$ sharing a common value of coefficients $\boldsymbol{\theta}^{(l)}(A)$. The parameter α is an unknown concentration parameter controlling the degree of clustering. The measure G_0 is a 'base' measure on $\boldsymbol{\theta}^{(l)}(A)$, which is assumed known, up to a finite-dimensional parameter. As the concentration parameter, α, tends to zero, a sampled distribution, G, from the DP prior is likely to be concentrated on a few points, resulting in few clusters. As α becomes large, a sampled distribution, G, will be very similar to the base distribution, G_0, so that samples from G will be, with high probability, distinct, resulting in a larger number of distinct clusters. See Escobar and West (1995) for a more in depth discussion. We specify G_0 to be a product of Gaussian distributions, $\mathrm{N}_p(\mathbf{0}, \sigma^2_{\boldsymbol{\beta}} \boldsymbol{I}_{p\times p})$ and $\mathrm{N}_r(\mathbf{0}, \sigma^2_{\boldsymbol{\eta}} \boldsymbol{K})$, on the $\boldsymbol{\beta}$ and $\boldsymbol{\eta}$ components of $\boldsymbol{\theta}$, respectively.

To complete the model specification, we need to choose prior distributions on the unknown parameters $\sigma^2_{\boldsymbol{\eta}}$ and α. We let $\sigma^2_{\boldsymbol{\eta}} \sim \mathrm{IG}(a_{\boldsymbol{\eta}}, b_{\boldsymbol{\eta}})$, and $\alpha \sim \mathrm{Gamma}(a_\alpha, b_\alpha)$, for fixed hyperparameters $a_{\boldsymbol{\eta}}, b_{\boldsymbol{\eta}}, a_\alpha$, and b_α. We generally set $a_{\boldsymbol{\eta}}$, $b_{\boldsymbol{\eta}}$, a_α and b_α to be small, positive constants, and $\sigma^2_{\boldsymbol{\beta}}$ to be a large number, giving vague, but proper priors on $\boldsymbol{\beta}$, α, and $\sigma^2_{\boldsymbol{\eta}}$. This choice of prior on the hyperparamters provides "low-information" and imparts little impact on the analysis.

This choice of parameter model, when combined with the data augmentation approach of Escobar and West (1995), gives full conditional distributions that are all from simple parametric families. Gibbs sampling can then be used to sample from the posterior distribution, using methods from Neal (2000). Computational details for the sampler can be found in the Supplementary Materials. Given draws $\boldsymbol{\theta}^{(l)}_r(A)$ for $r = 1, \ldots, R$ of $\boldsymbol{\theta}^{(l)}(A)$ from the sampler, draws $Y^{*(l)}(A)$ can be assembled via (5) and (8), and model-based predictions, variances, and standard errors of $Y^{*(l)}(A)$ can be produced using (7).

REMARK 4.1. While Gibbs sampling algorithms exist for the nonparametric Dirichlet process prior, the computational burden can be large for two main reasons. First, because the number of clusters is random in this model specification, there is potentially a large memory need, as parameter values need to be drawn and saved for each cluster, at each iteration of the Gibbs sampler. In particular, at early stages of the Gibbs sampler, there are often a large number of clusters that are investigated prior to convergence of the MCMC chain. Second, the number of iterations for convergence of the Gibbs sampler can be large, especially if the initial values of the unknown parameters are chosen poorly.

To speed up convergence, a parametric approximation to the Dirichlet process prior can be used. The Dirichlet process with base measure G_0 and concentration parameter α can alternatively be written as the random measure

$$\mathcal{P}(\cdot) = \sum_{k=1}^{\infty} \pi_k \delta_{\boldsymbol{\theta}_k}(\cdot), \tag{9}$$

known as the stick-breaking representation (Sethuraman, 1994). Here, the $\delta_{\boldsymbol{\theta}_k}(\cdot)$ are point masses concentrated on random variables $\boldsymbol{\theta}_k \overset{\text{i.i.d.}}{\sim} G_0$, and the $\pi_k = \phi_k \prod_{b=1}^{k-1}(1-\phi_b)$ are weights based on random variables $\phi_k \overset{\text{i.i.d.}}{\sim} \mathrm{Beta}(1, \alpha)$.

If there is a priori knowledge of a maximum number of clusters, the series (9) can be truncated to a number of terms, say M, which is greater than the known number of clusters. The truncated random measure

$$\mathcal{P}_M(\cdot) = \sum_{k=1}^{M} \pi_k \delta_{\boldsymbol{\theta}_k}(\cdot), \tag{10}$$

can be used as a parametric approximation to the Dirichlet process prior, and inference can be done using a Gibbs sampler, described in detail in Ishwaran and James (2001). ■

In practice, the choice of M and the number of basis functions is problem-specific. In general, we recommend choosing M large enough that number of times that the dimension M is visited in the Gibbs sampler is infrequent or not at all. Additionally, choosing the number of basis functions constitutes an open area of research, e.g., see Bradley, Cressie and Shi (2016) and the references therein. Our approach is to choose this number large enough that increasing the number of basis functions does not result in any appreciable difference in the resulting target estimates.

REMARK 4.2. In the experiments done in this paper, inference using the parametric approximation in (10) was very similar to inference using the exact Dirichlet process prior in (9), so long as the truncation level M was sufficiently large. If the maximum number of clusters, M, was chosen too small, we found the multivariate spatial mixture model, using the truncated measure (9) as a prior, had some of the same problems as the multivariate spatial model as was seen in Section 3.2. With the datasets studied in this paper, setting $M = 25$ worked well. The major advantage of using the prior (10) over the Dirichlet process prior is that the computational burden is greatly reduced. Both the memory requirements, and the computing time for convergence of the Gibbs sampler was much less, making use of (10) potentially more appealing for production of official estimates, particularly as the size of datasets and the number of datasets to analyze can be quite large. ■

REMARK 4.3. While our main focus is on producing area-level predictions with higher precision than the corresponding direct survey estimates, we are also interested in investigating the effectiveness of the clustering mechanism of the nonparametric spatial mixture model, and the degree to which the added model uncertainty of an unknown number of clusters affects the precision of the model-based predictions. The numerical example and data analysis in the following sections present results which use the multivariate spatial mixture with the nonparametric Dirichlet process (9) as a prior. ■

5. Empirical Simulation Study. In Section 3.2, we showed that the multivariate spatial model can produce predictions of areal quantities that are of obvious poor quality when there are varying spatial and multivariate patterns. We proposed an extension of the multivariate spatial model in Section 4, which clusters the data on these varying characteristics, by introducing a Dirichlet process prior on the process model. In this section we present results of a data-based, empirical simulation study, designed to study properties of this multivariate spatial mixture model (MSMM). The two main properties of interest are, first, to verify that the MSMM can effectively cluster data based on spatial patterns and multivariate properties of the data, and second, that the predictions at the areal level are more precise, on average, than the corresponding direct estimates. For comparison, we also show the performance of predictions using a Fay-Herriot model (Fay and Herriot, 1979), given by

$$
\begin{aligned}
Z^{(l)}(A) &= Y^{(l)}(A) + \varepsilon^{(l)}(A) \\
Y^{(l)}(A) &= \boldsymbol{x}^{(l)}(A)^{\top}\boldsymbol{\beta} + \nu^{(l)}(A),
\end{aligned} \tag{11}
$$

where $\varepsilon^{(l)}(A) \overset{\text{ind.}}{\sim} \mathrm{N}(0, D^{(l)}(A))$ and $\nu^{(l)}(A) \overset{\text{i.i.d.}}{\sim} \mathrm{N}(0, \sigma^2)$. The Fay-Herriot model (11) does not take into consideration any multivariate dependence or spatial dependence in the data, except for any information included in the covariates $\boldsymbol{x}^{(l)}(A)$.

REMARK 5.1. The multivariate spatial model, introduced in Section 2, was also fit to the simulated datasets. However, the performance of the predictions using this model are not shown, as these predictions suffer from the same problems as those discussed in Section 3.2. Primarily, the bias of the predictions in some areas is huge, making this model inappropriate for use with this type of data. ■

The simulation study is designed around the age by race dataset, discussed in Section 3.2, which could not be effectively modeled by the multivariate spatial model. Let $Z^{(l)}(A)$ represent the log of the direct ACS 5-year estimates of the counts, plus 1, given in equation (2), for each age by race cross-classification $l = 1, \ldots, 21$, in each of the counties, $A \in \mathcal{D}$, in Minnesota and surrounding states. Let $D^{(l)}(A)$ be the sampling variance of the $Z^{(l)}(A)$.

REMARK 5.2. The direct estimates of the counts, as in Equation (1), and their associated direct variance estimates are publicly available data. The U.S. Census Bureau uses the successive differences replication method (Judkins, 1990; Fay and Train, 1995; Torrieri, 2014) to create replicate weights for variance estimation. These replicate weights can also be used to estimate the variance of the direct estimates of the log counts; these are the variance estimates that are used in Section 6. However, the variance estimates of the log counts are not publicly available data. In order to present results of a numerical example based completely on publicly available data, we instead use the delta method to transform the variance estimates from the count scale to the log count scale, and then smooth the transformed estimates so they more closely agree with the replicate weight variance estimates. Details can be found in the Supplementary Materials. ■

The perturbed version of the log counts is

$$R^{(l)}(A) = Z^{(l)}(A) + \varepsilon^{(l)}(A),\ l = 1, \ldots, 21,\ A \in \mathcal{D}, \tag{12}$$

where $\varepsilon^{(l)}(A) \overset{\text{ind.}}{\sim} \mathrm{N}(0, D^{(l)}(A))$. In this setup, the $D^{(l)}(A)$ are used as the sampling variance of the log counts, $R^{(l)}(A)$, and are assumed known. For the purpose of this empirical study, we act as if the direct estimates of the log counts, $Z^{(l)}(A)$, are the unobserved, true multivariate spatial latent process, and treat the $R^{(l)}(A)$ as the data process. This empirical simulation study is similar to what is done in Bradley, Holan and Wikle (2015) and Bradley, Holan and Wikle (2018), and is designed as a way of generating data that behave similar to what might be observed in practice.

We generate 100 datasets from (12), giving us "observed" values $\{(R^{(l)}(A), D^{(l)}(A))\}$. The MSMM is fit to the perturbed values $R^{(l)}(A)$ in each simulated dataset to predict the $Z^{(l)}(A)$. The covariates used in the model include an intercept, the log of the total county population (which is assumed known from Census data), and a collection of dummy variables corresponding to the different age by race cross-classifications. The hyperparameters used were $a_{\boldsymbol{\eta}} = b_{\boldsymbol{\eta}} = 0.1$, $\sigma^2_{\boldsymbol{\beta}} = 100$, $a_\alpha = 1$ and $b_\alpha = 4$. These hyperparameters give vague, but proper priors, on $\boldsymbol{\beta}$ and σ^2_η. Since, with the Dirichlet process, the number of clusters is asymptotically equal to $\alpha \log n$ (Korwar and Hollander, 1973), we chose the hyperparameters $a_\alpha = 1$ and $b_\alpha = 4$ put prior mass on smaller values of α, with 90% of the prior mass on $(0.2, 1)$, giving prior preference to a smaller number of clusters. We investigated different values of a_α and b_α, and did not find much sensitivity to the choice of hyperparameters, except for the amount of time to reach convergence, and the number of clusters which were created at early iterations of the Gibbs sampler.

For each simulated dataset $i = 1, \ldots, 100$, the MSMM was fit to the perturbed data, $\{R_i^{(l)}(A)\}$ using a Gibbs sampler whose derivation and computational details can be found

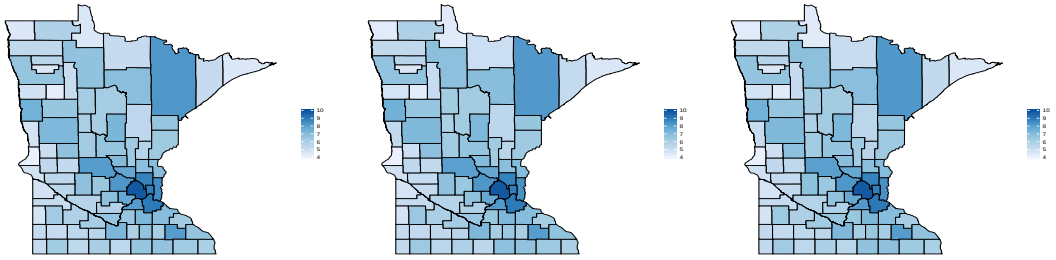

(a) "True" values of the log count of White children, ages 2–3

(b) Direct estimates of the log count of White children, ages 2–3

(c) Model-based predictions of the log count of White children, ages 2–3

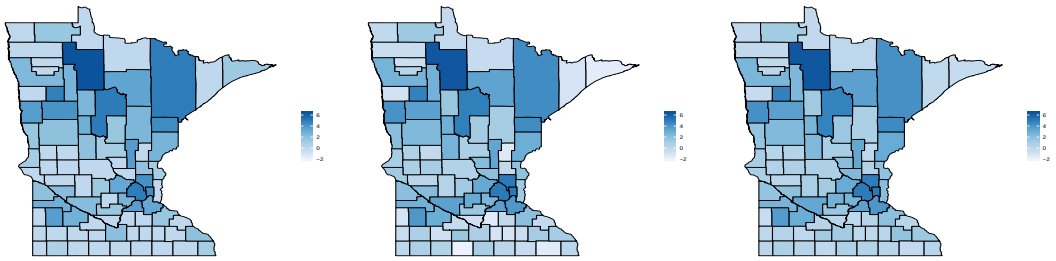

(d) "True" values of the log count of American Indian or Alaska Native children, ages 2–3.

(e) Direct estimates of the log count of American Indian or Alaska Native children, ages 2–3.

(f) Model-based predictions of the log count of American Indian or Alaska Native children, ages 2–3.

Fig 7: True values of the log count, perturbed values of the log count, and model based predictions of the log count, using the multivariate spatial mixture model. The first row shows these quantities for White children, ages 2–3, and the second row shows these quantities for American Indian or Alaska Native children, ages 2–3, in counties in Minnesota.

in the Supplementary Materials. The sampler was run for 5,000 iterations, with a burn-in of 1,000 iterations. Assessing convergence of the Gibbs sampler is challenging in the mixture model framework, due to potential label-switching. At each iteration of the MCMC chain, the number of clusters can change, and the associated cluster labels are arbitrary and change from iteration to iteration. We can, however, monitor the MCMC chains of parameters that are not dependent on the cluster labels, such as the concentration parameter, α, the variance parameters, $\sigma^2_{\boldsymbol{\beta}}$ and $\sigma^2_{\boldsymbol{\eta}}$, as well as predicted values of areal quantities which are invariant to label-switching. From this assessment, there was no lack of convergence detected, based on visual inspection of the MCMC chains for these parameters. Additionally, batch means (Jones et al., 2006), using the square root rule, and the Geweke statistic (Geweke, 1992), were computed as formal tests of MCMC convergence. Neither of these diagnostics indicated lack of convergence.

Let $\{\hat{Z}_i^{(l)}(A)\}$ denote the model-based predicted values of the log counts, $Z^{(l)}(A)$, from fitting the MSMM model to the ith simulated dataset for $i = 1, \ldots, 100$. In Figure 7 we show the "true" values of the log counts for counties in Minnesota for two margins: the log of the number of White children, ages 2–3, and the log of the number of American Indian or Alaska Native children, ages 2–3. Also shown are the perturbed data from the first simulation, as well as the predicted values of the log counts using the MSM mixture model fit to this perturbed dataset.

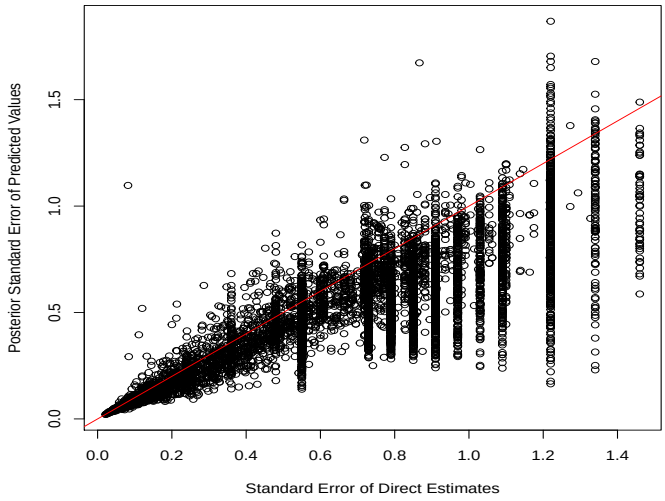

Fig 8: Posterior standard error of predicted values vs. design-based standard error of the direct estimates in Simulation 1.

Figure 7 highlights the difficulty of fitting a spatial model to this dataset. Both the "true" values, and the perturbed estimates exhibit very different spatial patterns for the different margins, White children ages 2–3, and American Indian or Alaska Native children, ages 2–3. Recall that the largest numbers of White children are in Hennepin county, which includes Minneapolis, and the largest number of American Indian or Alaska Native children are located in the more rural Beltrami County in the northern part of the state. However, predictions made using the multivariate spatial mixture model are able to largely preserve the spatial patterns in the margins of the dataset, in contrast to predictions made using the multivariate spatial model. Also, the predicted values are very close to the corresponding direct estimates when the area-specific sample size is very large (or equivalently, when the variance of the direct estimate is very small). For areas with smaller sample size, the direct estimates lack precision, and the model-based predictions "borrow strength", by exploiting multivariate and spatial dependence in the data, which is an important property of general small area estimates.

Figure 8 compares standard error of the predicted values of the log counts, estimated using the standard error of the posterior distribution, to the design-based standard errors of the pseudo data from the first simulated dataset, over all counties $A \in \mathcal{D}$ for all age by race cross-classifications. This is the usual way the precision of model-based estimates using hierarchical Bayesian methods is compared to the precision of design-based estimates in the small area estimation literature (Rao and Molina, 2015, Chapter 10).

From Figure 8, on average, and for the majority of the individual areas, we can see greatly reduced standard errors of the predicted values compared to the standard errors of the direct estimates, which is a primary goal (James and Stein, 1961; Fay and Herriot, 1979). There are, however, some areas where the standard error of predicted values increased, and a few of these increases are quite large.

A closer investigation of the predictions with large increases in standard error can be done by looking at their traceplots and their cluster memberships over the iterations of the Gibbs sampler. In these traceplots, it can be seen that these values do not settle into a single cluster with high probability, but instead switch between multiple clusters. This has the effect of

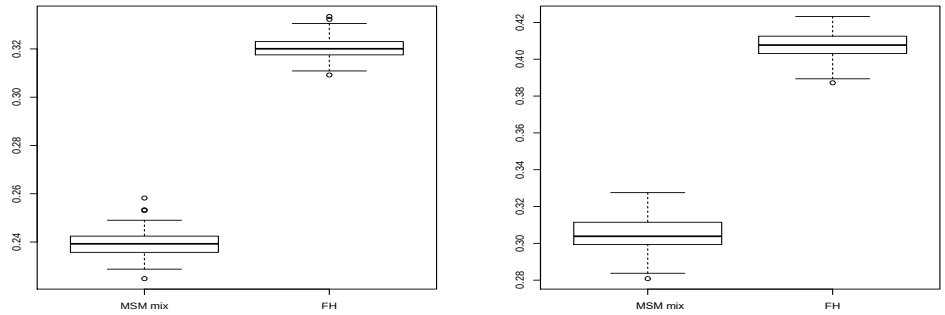

(a) Median absolute bias.

(b) Average mean squared error.

Fig 9: Boxplots of the median absolute bias MAB_i and the average mean squared error AMSE_i for simulation runs $i = 1, \ldots, 100$ from the model-based predictions using the MSM model and the Fay-Herriot model. For comparison, the average design-based variance of the direct estimates is 0.54.

limiting the bias of the predictions, but causes increased variability. In the analysis of this dataset, this seems to happen relatively infrequently.

Despite these few 'outlier' values in Figure 8, it is clear that the MSMM can effectively cluster the data based on the different spatial patterns and multivariate characteristics of the data, and can produce predictions which preserve the spatial characteristics of the data and can exploit spatial and multivariate dependencies so that the precision of the predictions is greatly increased over the precision of the direct estimates, for the majority of the areas.

The overall performance of the predictions using the MSMM can be evaluated by comparing the predicted values to the true values over the 100 simulations. First, the median absolute bias, given by

$$\text{MAB}_i = \text{median}\left\{\left|\hat{Z}_i^{(l)}(A) - Z_i^{(l)}(A)\right| : A \in \mathcal{D}, l = 1, \ldots, L\right\},$$

is evaluated over the 100 simulations used for predictions using both the MSMM, as well as predictions using the Fay-Herriot model. Figure 9a shows a boxplot of the median absolute bias of predictions from the MSMM compared to the median absolute bias of predictions from the Fay-Herriot model. From 9a, we see that the MSMM produces predictions with reduced absolute bias compared to predictions from the Fay-Herriot model. We also compute the average mean squared error (MSE), given by

$$\text{AMSE}_i = \frac{1}{n}\sum_{l=1}^{L}\sum_{A\in\mathcal{D}}\left(\hat{Z}_i^{(l)}(A) - Z_i^{(l)}(A)\right)^2.$$

Figure 9b shows a boxplot of the average MSE of predictions from the MSMM compared to the average MSE of predictions from the Fay-Herriot model. For comparison, the average design-based variance of the direct estimates is 0.54. While predictions made using Fay-Herriot model are, on average, more precise that the direct estimates, the gain in precision is modest. It is clear from Figure 9b, that the multivariate and spatial dependence in the data can be used to greatly improve the MSE of predicted values.

6. Estimates of the number of children by race and ethnicity in counties in Minnesota using the multivariate spatial mixture model. In Section 3.2, we fit the multivariate spatial model to the age by race dataset, and found that many model-based predictions were

TABLE 1

A selection of the direct estimates and their estimated standard errors of the counts of persons by age and race in counties in the Midwestern states surrounding Minnesota. The Order column indexes the 21 age by race categories. The full dataset consists of 7896 rows.

State	County	Order	Count	Std. Err.
19	041	1	325	49.2
19	041	2	370	48.0
19	041	3	375	49.9
⋮	⋮	⋮	⋮	⋮
46	123	19	4	3.6
46	123	20	15	14.0
46	123	21	15	14.0

unreasonable. We hypothesized that the cause of these unrealistic predictions was the presence of multiple spatial fields within the margins of the multivariate data. In this situation, it seems plausible that when a model with a single spatial field is specified, and estimated from the data, that predictions based on the single spatial field can be too drastically distorted from the direct estimates, when in truth there are multiple underlying spatial patterns.

In this section, we fit the MSMM to the ACS dataset considered in Section 3.2 to obtain model-based predictions of counts by age and race in counties in Minnesota. A partial table of the data is shown in Table 1. The data is presented using FIPS codes for the 376 counties within Minnesota and the surrounding Midwestern states (North Dakota, South Dakota, Wisconsin, and Iowa).

Figure 6 shows the spatial patterns of the direct estimates within counties in Minnesota for two margins of the data. Figure 6a shows the direct estimates of the number of White children, ages 2–3, and Figure 6b shows the direct estimates of the number of American Indian or Alaska Native children, ages 2–3. Exploratory analysis of each of the margins of the data indicate strong spatial correlation using Moran's I statistic (Moran, 1950). However, clearly the spatial patterns across different margins can be quite different. The different ranges of the data within the different margins (0–700 in Figure 6a and 0–16,000 in Figure 6b) pose an additional challenge. As was seen in Section 3.2, using a multivariate spatial model with a common spatial field for all margins of the data for difficult datasets such as this one can result in predictions which are nonsensical for certain areas, due to the aggressive smoothing from the common fitted spatial field.

To account for the varying spatial patterns in this dataset, we fit the MSMM to the log of the direct estimates, plus 1, as in Equation (2). This allows for clustering of the data by common spatial and multivariate characteristics. It also makes it possible to obtain model-based predictions which are improvements over the corresponding direct estimates, by exploiting the multivariate dependence and the spatial dependence within the data. This is of particular importance in the situation where there is limited covariate information which can be used for prediction.

The design-based variance of the log transformed direct estimates was estimated using the method of replicate weights (Judkins, 1990), when these quantities were well defined. For the remaining areas, the variance estimates were imputed, using predictions from a LOESS regression, as was done in Section 3.1. These variance estimates (not shown, as these are not publicly available data) are used in the data model, and are treated as known quantities. The covariates, basis functions, and hyperparameters used were the same as described in Section 5.

The MCMC algorithm was run for 10,000 iterations, with the first 5,000 iterations discarded. As the parameters of interest are the finite population totals, exponential transformation (5) is applied to the model-based predictions (which have been computed at the log

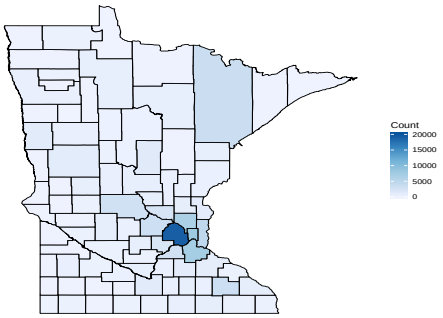

(a) Direct estimates of the number of White children, ages 2–3.

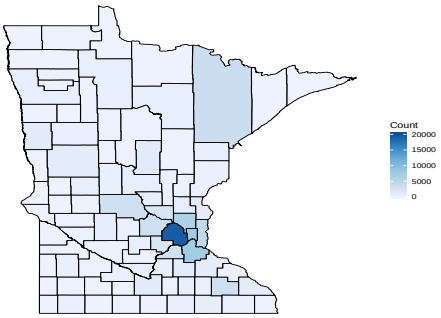

(b) Model-based predictions of the number of White children, ages 2–3.

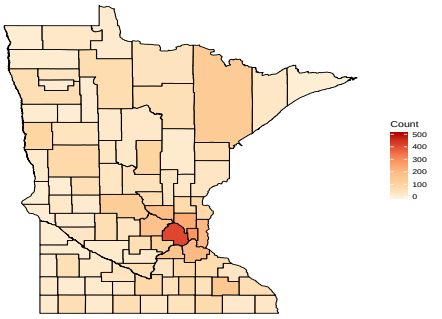

(c) Standard errors of direct estimates of the number of White children, ages 2–3.

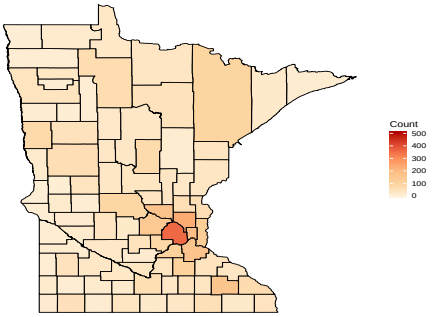

(d) Posterior standard error of model-based predictions of the number of White children, ages 2–3.

Fig 10: Comparison of the spatial patterns of the direct estimates and the predicted values of the number of White children, ages 2–3, in blue, and a comparison of the spatial patterns of the standard errors of the direct estimates and predicted values, of the number of White children, ages 2–3, in red.

scale) for each iteration of the MCMC chain. Two parallel MCMC chains were run, which allows for convergence checks on the parameters α and $\sigma^2_{\boldsymbol{\eta}}$, which are not dependent on cluster labels. There was no lack of convergence detected based on visual inspection of the MCMC chains for these parameters, nor was there any indication of convergence issues based on the batch means, Geweke statistic (Geweke, 1992), or the Gelman Rubin statistics (Gelman and Rubin, 1992). The computational time to run 10,000 MCMC iterations using a single processor and 25GB of RAM on a linux server was approximately 14 hours.

All predictions presented here are of aggregated quantities at the county level, which are invariant to cluster permutations, so we were able to present results without concern about any possible issues due to label switching. However, if inference on marginal posterior quantities, such as cluster membership, is of interest, it is crucial to post-process the estimates using an algorithm to correct for label switching, for example using the results of Stephens (2000).

The nonparametric Dirichlet prior was incorporated into the multivariate spatial mixture model, in part, to allow the 'true' number of clusters to be an unknown quantity. We note that the posterior modal number of clusters is 8, with a posterior standard error of 1, with nearly

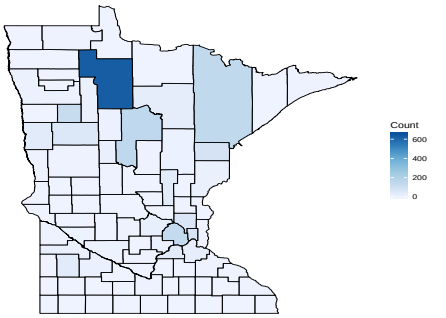

(a) Direct estimates of the number of American Indian or Alaska Native children, ages 2–3.

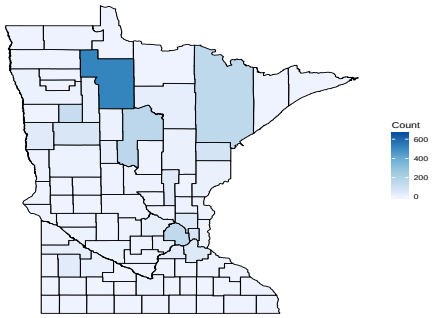

(b) Model-based predictions of the number of American Indian or Alaska Native children, ages 2–3.

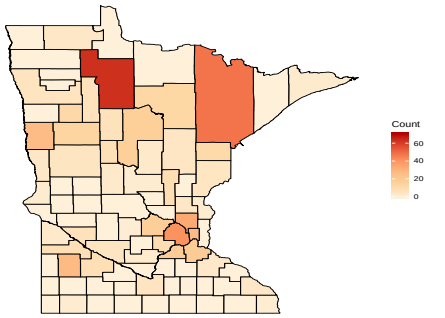

(c) Standard errors of direct estimates of the number of American Indian or Alaska Native children, ages 2–3.

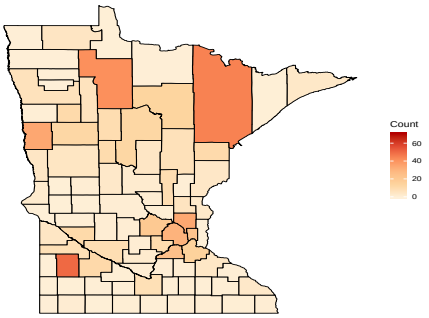

(d) Posterior standard error of model-based predictions of the number of American Indian or Alaska Native children, ages 2–3.

Fig 11: Comparison of the spatial patterns of the direct estimates and the predicted values of the number of American Indian or Alaska Native children, ages 2–3, in blue, and a comparison of the spatial patterns of the standard errors of the direct estimates and predicted values, of the number of American Indian or Alaska Native children, ages 2–3, in red.

all of the drawn number of clusters within ± 2 of the posterior mode. Recall that there are 21 (3 age and 7 race) observations per county. The effectiveness of the clustering mechanism can be seen in Figures 10 and 11. Figure 10 gives a comparison of the direct estimates and their associated variance estimates with the model-based predictions of the county-level counts of White children, ages 2 – 3, and their posterior variances. Here, we see similar spatial patterns of both the direct estimates and the model-based predictions. We also see the overall reduction in standard errors in Figures 10c and 10d.

Figure 11 gives a comparison of the direct estimates and their associated variance estimates with the model-based predictions of the county-level counts of American Indian or Alaska Native children, ages 2–3, and their posterior variances. A comparison of Figure 11 with Figure 10 highlights the ability to preserve multiple spatial patterns within a given dataset when using predictions from the multivariate spatial mixture model. A comparison of the standard errors of the direct estimates with the posterior standard errors of the model-based predictions is made in Figures 11c and 11d. For the majority of the counties in Minnesota, the

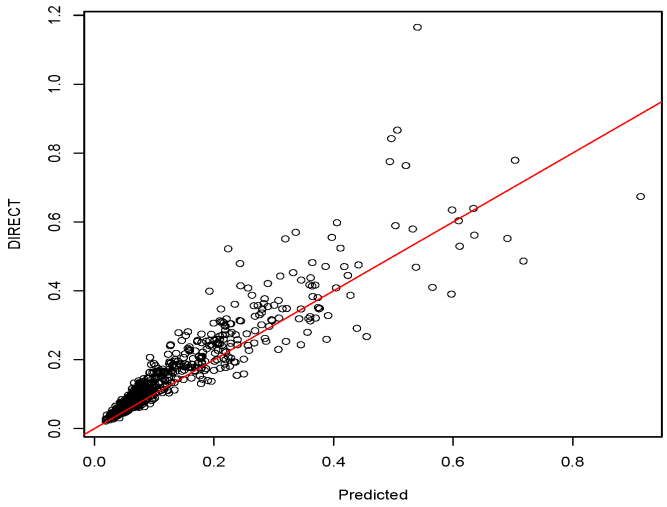

Fig 12: Comparison of the coefficients of variation of the predicted values vs. the coefficients of variation of the direct estimates. The diagonal line is shown in red.

posterior standard errors of the model-based predictions were lower than the corresponding standard errors of the direct estimates. However, for a few of the counties, there was a slight increase in the estimated standard error.

The overall performance of the uncertainty estimates is presented in Figure 12, which shows a scatter plot of the coefficients of variation of the direct estimates against the coefficients of variation of the predicted values among the set of nonzero direct estimates. Figure 12 gives a similar result to what was seen in the empirical simulation study in Section 5. Overall, the precision of the model-based predictions is greater than that of the direct estimates. However, there are some counties which had an increase in their coefficient of variation, due to the parameter values associated with that county switching between clusters at different iterations of the MCMC chain. This cluster jumping seems to reduce the bias of the predictions, but can increase variability for some areas. Additional graphical comparisons of the direct estimates to model-based predictions using the multivariate spatial mixture model can be found in the Supplementary Materials.

While we do see an overall average reduction in the coefficients of variation and posterior standard errors of the model-based predictions over those corresponding to the direct estimates, the reductions are not as dramatic as was seen when fitting the multivariate spatial model to the simpler dataset analyzed in Section 3.1. Also, we do not achieve uniform reductions in coefficients of variation or standard errors, as there can be increases in these quantities in individual counties. Neither of these observations is surprising, as the age by race by county ACS dataset is of higher dimension and less well behaved than the age by county dataset. Likewise, the multivariate spatial mixture model needed to analyze the age by race dataset is far more complex than the multivariate spatial model. Despite these challenges, the multivariate spatial mixture model is promising as a tool for analyzing high dimensional survey data with varying spatial and multivariate characteristics. This model seemed to effectively cluster the age by race dataset in such a way as to preserve spatial patterns in the data, as well as to produce more precise predictions, on average, than the corresponding direct estimates.

7. Conclusion. Model-based estimation of area-level tabulations from the ACS is a challenging problem at the sub-state level when simultaneously considering other detailed demographic factors. Motivated by the need to produce special tabulations for the ACS, this paper introduces a nonparametric Bayesian multivariate spatial mixed effects model. As demonstrated in Sections 5 and 6, the proposed model provides a solution to an important problem encountered at the U.S. Census Bureau and is of independent interest.

When disseminating model-based estimates (model-based special tabulations) it is critical that the estimates retain the spatial patterns found in the observed sample and significantly improve the precision over the direct estimates. Additionally, the model needs to be flexible, in that it is effective across a wide range of problems without requiring subject matter expertise to propose new model variants for each dataset considered. These aspects are achieved by our proposed approach.

Notably, our model is nonparametric Bayes. For extremely high-dimensional settings, we consider an approximation that uses a finite representation through a stick-breaking prior. The latter approach may be preferable in a production setting at federal statistical agencies, as this can improve the computational efficiency without significant loss in precision.

In practice, the models introduced herein are initially developed for each special tabulation use case using the general model structure we propose. Subsequently, we envision the models will be rerun annually as new data are collected. This differs slightly from annually running a general model to the multitude of tabulations that the ACS produces. Even in the case of using the stick-breaking prior, convergence and goodness-of-fit will need to be monitored. Nevertheless, the stick-breaking prior is computationally advantageous and will, thus, broaden the applicability of the proposed approach to a wider array of use cases.

The approach considered here is conducted at the area level. Nevertheless, official statistical agencies have access to the underlying confidential micro-data (unit-level). One area of future research is to extend this approach to the unit-level. To do this in the context of ACS would require methodology that accommodates the informative sampling mechanism.

Acknowledgements. The DRB approval number for this paper is CDBRB-FY20-044. This report is released to inform interested parties of ongoing research and to encourage discussion of work in progress. The views expressed are those of the authors, and not those of the U.S. Census Bureau.

SUPPLEMENTARY MATERIAL

Supplementary Materials for Bayesian Nonparametric Multivariate Spatial Mixture Mixed Effects Models With Application to American Community Survey Special Tabulations. The supplementary material contains additional details on model specifications, as well as derivations of the full conditional distributions needed for the Gibbs sampler for posterior inference, for both the multivariate spatial model, as well as the multivariate spatial mixture model, introduced in the main paper. In addition, computational details for efficient construction of the multivariate spatial basis functions and the precision matrix of the latent Gaussian process are provided. Also, additional information about the variance estimates of the log-transformed direct estimates used in the numerical examples is given.

Code. There are four R scripts included in the Supplementary Materials, and one Stan script. The file fh-msm.stan contains the Stan model for fitting the multivariate spatial mixture model in Section 2. The file msmix-dp.R contains the Gibbs sampler for the multivariate spatial mixture model in Section 4. The file msmix-sb.R contains the Gibbs sampler for the stick-breaking version of the multivariate spatial mixture model. The file fit-model.R gives a workflow for fitting the multivariate spatial mixture model to the age by race dataset, and can

be used to reproduce the results of the empirical simulation study in Section 5. Finally, the file sim_summary.R contains the code used to summarize the output of the Gibbs sampler.

Dataset. The file dat_sf_sim_new.rds contains an R data frame, which includes the direct estimates, design-based estimates of their standard errors, the log-transformed direct estimates, and a smoothed version of their design-based standard errors using the Delta method, used in Sections 3.2, 5, and 6. This dataset contains the county-level data for Minnesota and the surrounding Midwestern states.
().

REFERENCES

ABOWD, J. M. (2018). The US Census Bureau adopts differential privacy. In *Proceedings of the 24th ACM SIGKDD International Conference on Knowledge Discovery & Data Mining* 2867–2867.

BANERJEE, S., CARLIN, B. P. and GELFAND, A. E. (2014). *Hierarchical Modeling and Analysis for Spatial Data*, 2nd ed. Chapman and Hall/CRC.

BRADLEY, J. R., CRESSIE, N. and SHI, T. (2016). A comparison of spatial predictors when datasets could be very large. *Statistics Surveys* **10** 100–131.

BRADLEY, J. R., HOLAN, S. H. and WIKLE, C. K. (2015). Multivariate spatio-temporal models for high-dimensional areal data with application to Longitudinal Employer-Household Dynamics. *Annals of Applied Statistics* **9** 1761–1791.

BRADLEY, J. R., HOLAN, S. H. and WIKLE, C. K. (2018). Computationally Efficient Multivariate Spatio-Temporal Models for High-Dimensional Count-Valued Data. *Bayesian Analysis* **13** 253–310.

BRADLEY, J. R., WIKLE, C. K. and HOLAN, S. H. (2017). Regionalization of multiscale spatial processes by using a criterion for spatial aggregation error. *Journal of the Royal Statistical Society: Series B (Statistical Methodology)* **79** 815–832.

CRESSIE, N. and WIKLE, C. (2011). *Statistics for Spatio-Temporal Data*. John Wiley & Sons.

DIGGLE, P. J., TAWN, J. A. and MOYEED, R. A. (1998). Model-based geostatistics. *Journal of the Royal Statistical Society: Series C (Applied Statistics)* **47** 299–350.

DUAN, J. A., GUINDANI, M. and GELFAND, A. E. (2007). Generalized spatial Dirichlet process models. *Biometrika* **94** 809–825.

ESCOBAR, M. D. and WEST, M. (1995). Bayesian density estimation and inference using mixtures. *Journal of the American Statistical Association* **90** 577 – 588.

FAY, R. and HERRIOT, R. (1979). Estimates of income for small places: an application of James-Stein procedures to Census data. *Journal of the American Statistical Association* **74** 269 - 277.

FAY, R. and TRAIN, G. (1995). Aspects of survey and model based postcensal estimation of income and poverty characteristics for states and counties. In *Joint Statistical Meetings: Proceedings of the Section of Government Statistics* 154-159.

FERGUSON, T. S. (1973). A Bayesian analysis of some nonparametric problems. *The Annals of Statistics* **1** 209 – 230.

FERNÁNDEZ, C. and GREEN, P. J. (2002). Modelling spatially correlated data via mixtures: a Bayesian approach. *Journal of the royal statistical society: series B (Statistical methodology)* **64** 805–826.

GELFAND, A. E., KOTTAS, A. and MACEACHERN, S. N. (2005). Bayesian nonparametric spatial modeling with Dirichlet process mixing. *Journal of the American Statistical Association* **100** 1021 – 1035.

GELMAN, A. and RUBIN, D. B. (1992). Inference from iterative simulation using multiple sequences. *Statistical Science* **7** 457 – 472.

GEWEKE, J. (1992). Evaluating the accuracy of sampling-based approaches to the calculation of posterior moments (with discussion). In *Bayesian Statistics 4: Proceedings of the Fourth Valencia International Meeting* (J. M. Bernardo, J. O. Berger, A. P. Dawid and A. F. M. Smith, eds.) 169 - 193. Oxford University Press.

HIGHAM, N. J. (1988). Computing a nearest symmetric positive semidefinite matrix. *Linear Algebra and its Applications* **103** 103–118.

HJORT, N. L., HOLMES, C., MÜLLER, P. and WALKER, S. G. (2010). *Bayesian Nonparametrics* **28**. Cambridge University Press.

HOSSAIN, M. M., LAWSON, A. B., CAI, B., CHOI, J., LIU, J. and KIRBY, R. S. (2013). Space-time stick-breaking processes for small area disease cluster estimation. *Environmental and ecological statistics* **20** 91–107.

HOSSEINPOURI, M. and KHALEDI, M. J. (2019). An area-specific stick breaking process for spatial data. *Statistical Papers* **60** 199–221.

HUGHES, J. and HARAN, M. (2013). Dimension reduction and alleviation of confounding for spatial generalized linear mixed models. *Journal of the Royal Statistical Society, Series B* **75** 139 - 159.

ISHWARAN, H. and JAMES, L. F. (2001). Gibbs sampling methods for stick-breaking priors. *Journal of the American Statistical Association* **96** 161 – 173.

JAMES, W. and STEIN, C. (1961). Estimation with quadratic loss. In *Proceedings of the 4th Berkely Symposium on Mathematical Statistics and Probability* 361 - 379. University of California Press, Berkeley.

JONES, G. L., HARAN, M., CAFFO, B. S. and NEATH, R. (2006). Fixed-width output analysis for Markov chain Monte Carlo. *Journal of the American Statistical Association* **101** 1537 - 1547.

JUDKINS, D. R. (1990). Fay's method for variance estimation. *Journal of Official Statistics* **6** 223 - 239.

KORWAR, R. M. and HOLLANDER, M. (1973). Contributions to the theory of Dirichlet processes. *Annals of Probability* **1** 705 - 711.

KOTTAS, A. (2016). Bayesian nonparametric modeling for disease incidence data. *Handbook of spatial epidemiology. Chapman and Hall/CRC, London* 363–374.

MOLINA, I., NANDRAM, B. and RAO, J. N. K. (2014). Small area estimation of general parameters with application to poverty indicators: A hierarchical Bayesian approach. *Annals of Applied Statistics* **8** 852 – 885.

MORAN, P. A. P. (1950). Notes on continuous stochastic phenomena. *Biometrika* **37** 17 – 23.

NEAL, R. M. (2000). Markov chain sampling methods for Dirichlet process mixture models. *Journal of Computational and Graphical Statistics* **9** 249 – 265.

NEELON, B., GELFAND, A. E. and MIRANDA, M. L. (2014). A multivariate spatial mixture model for areal data: examining regional differences in standardized test scores. *Journal of the Royal Statistical Society. Series C, Applied statistics* **63** 737.

PORTER, A. T., HOLAN, S. H. and WIKLE, C. K. (2015). Bayesian semiparametric hierarchical empirical likelihood spatial models. *Journal of Statistical Planning and Inference* **165**.

QIU, Y. and MEI, J. (2019). RSpectra: Solvers for Large-Scale Eigenvalue and SVD Problems R package version 0.16-0.

RAO, J. N. K. and MOLINA, I. (2015). *Small Area Estimation*, second ed. John Wiley & Sons, Inc.

REICH, B. J. and FUENTES, M. (2015). Spatial Bayesian nonparametric methods. In *Nonparametric Bayesian Inference in Biostatistics* 347–357. Springer.

SETHURAMAN, J. (1994). A constructive definition of Dirichlet priors. *Statistica Sinica* **4** 639 – 650.

STEPHENS, M. (2000). Dealing with label switching in mixture models. *Journal of the Royal Statistical Society, Series B* **62** 795 - 809.

STAN DEVELOPMENT TEAM (2018). RStan: the R interface to Stan.

R CORE TEAM (2019). R: A Language and Environment for Statistical Computing R Foundation for Statistical Computing.

TORRIERI, N. (2014). American Community Survey Design and Methodology Technical Report, United States Census Bureau.